

Cite this: *Chem. Sci.*, 2015, **6**, 3373

Received 26th February 2015

Accepted 2nd April 2015

DOI: 10.1039/c5sc00720h

www.rsc.org/chemicalscience

## Introduction

Nitrite reductases (NiRs) are enzymes found in prokaryotic organisms which catalyze the one-electron ( $e^-$ ) reduction of nitrite to nitric oxide (NO).<sup>1</sup> Copper nitrite reductases (CuNiRs) are homotrimeric enzymes with each monomer containing two copper centers: a T1 site for electron transfer, and a catalytically-active T2 site.<sup>2</sup> Although X-ray crystallographic studies have provided structural snapshots of intermediates along the reduction pathway,<sup>3</sup> the precise mechanism by which CuNiR catalyzes nitrite reduction has been disputed.<sup>1c</sup> In one proposed pathway, nitrite coordinates to the reduced T2 center, then following two proton ( $H^+$ ) transfer events, water is released and a copper-nitrosyl species is generated (described as either Cu(i)-NO<sup>+</sup> or Cu(ii)-NO); Fig. 1A.<sup>3c,4</sup> In support of this mechanism, a crystal structure of CuNiR with NO bound to the reduced T2 site was reported with an unusual side-on binding mode of NO,<sup>5</sup> which suggests that NO coordination to copper is at least possible under reducing conditions.<sup>6</sup> However, an oxidized Cu(NO) unit (*i.e.* Fig. 1A) would be capable of nitrosylating nearby amino acid residues,<sup>7</sup> and thus is unlikely to be formed under catalytic conditions. An alternative pathway for nitrite reduction catalyzed by CuNiR has been described wherein nitrite first coordinates to the oxidized T2 center followed by  $H^+$  transfer from a nearby aspartic acid residue to protonate the coordinated nitrite.<sup>8</sup> In this case, protonation of nitrite triggers  $e^-$  transfer from the T1 center to the T2 center, with release of NO to form a copper-hydroxide (Fig. 1B). This mechanism is consistent with isolated crystal structures of CuNiR with nitrite bound to the oxidized T2 center,<sup>3c</sup> steady-state kinetics and pulsed radiolysis experiments,<sup>9</sup> and computational modeling.<sup>10</sup> Although the intimate pathway of nitrite reduction may be

disputed, the network of hydrogen bonds (H-bonds) provided by nearby amino acid residues is widely accepted to play a key role in positioning substrate and facilitating  $e^-$  transfer.<sup>1c</sup>

With the goal of clarifying the fundamental pathways of nitrite reduction, the reactivity of synthetic copper complexes toward nitrite has been extensively studied,<sup>1c</sup> although limited examples have been reported that demonstrate secondary sphere interactions with a copper nitrite complex.<sup>11</sup> Prior reports have largely focused on the preparation of copper(i) nitrite adducts and subsequent reactivity with exogenous  $H^+$  sources to release NO. One critical distinction between synthetic copper(i) nitrite adducts and CuNiR is the observed mode of nitrite coordination: there are no reported synthetic copper(i) complexes supported by biologically-relevant ligands that feature the  $\kappa$ O-nitrite coordination observed in CuNiR, and instead exclusively feature  $\kappa$ N-coordination.<sup>12</sup>

While select systems have been shown to produce NO from a copper(i) nitrite complex,<sup>1c,13</sup> the mechanism by which these reactions proceed are often not fully resolved, thus precluding direct mechanistic comparisons to CuNiR. One reason for limited mechanistic insight has been the isolation of terminal copper(ii) complexes which do not contain the inorganic products of nitrite reduction (*i.e.*  $H_2O$  or NO).<sup>13b,13d,13f</sup> Although copper(ii)-nitrosyls have been implicated in many synthetic nitrite reduction pathways, their isolation has remained elusive,<sup>7b,14,15</sup> thus calling into question their role in synthetic and biological copper nitrite reduction schemes.

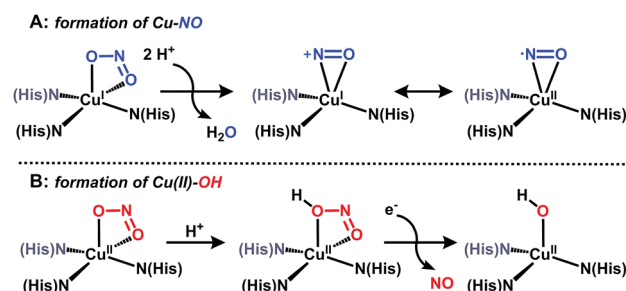


Fig. 1 Postulated intermediates for nitrite reduction by CuNiR.

Department of Chemistry, University of Michigan, 930 N. University Ave., Ann Arbor, MI 48109, USA. E-mail: nszym@umich.edu

† Electronic supplementary information (ESI) available: Synthetic and experimental procedures, spectral data and computational details. CCDC 1051416 and 1056984. For ESI and crystallographic data in CIF or other electronic format see DOI: 10.1039/c5sc00720h

A nitrite reduction pathway that circumvents the formation of a highly reactive copper–nitrosyl species is likely operative in CuNiR (Fig. 1B). In this Edge Article, we demonstrate that nitrite reduction by a copper complex supported by a proton-responsive ligand proceeds through a parallel pathway. A mechanism is described whereby a  $H^+/e^-$  transfer pathway to nitrite releases NO, which bypasses the formation of an unstable copper(II)–nitrosyl species, and provides a synthetic mechanistic analogue for nitrite reduction in CuNiR.

## Results and discussion

Recently we described copper complexes supported by  $H_3\text{thpa}$ , a tripodal ligand featuring pendent hydroxyl groups capable of engaging in H-bonding interactions with metal bound substrates.<sup>16</sup> We previously showed that the H-bonding manifold presented by  $H_3\text{thpa}$  allows access to a unique copper(I) fluoride complex ( $\text{CuF}(H_3\text{thpa})$ , **1**) that is best described as containing a ‘captured’ fluoride anion in the secondary coordination sphere.<sup>16b</sup> We envisioned that anions capped by  $\text{SiR}_3^+$  units would react with **1** via metathesis to provide new copper complexes in which we could interrogate H-bonding and  $H^+/e^-$  transfer reactivity toward reducible substrates. Specifically, we sought to exploit this methodology to examine the reactivity of **1** with nitrite in an effort to experimentally distinguish between two mechanistic pathways of nitrite reduction. Given the capability of the  $H_3\text{thpa}$  ligand scaffold to deliver  $H^+$  and subsequently provide H-bond donors and acceptors, we hypothesized that the inorganic products of nitrite reduction would be captured within a hydrogen bonding network surrounding the copper center.

In order to assess the ability of **1** to engage in metathesis reactivity with silyl-anions, we first examined the substitution of the fluoride anion in **1** for chloride. When **1** was treated with an equivalent of  $\text{Ph}_3\text{SiCl}$  at room temperature, the previously described  $\text{CuCl}(H_3\text{thpa})$ <sup>16a</sup> complex and  $\text{Ph}_3\text{SiF}$  were generated quantitatively; both of which were confirmed by  $^1\text{H}$  and  $^{19}\text{F}$  NMR spectroscopy (Fig. S1 and S2†). Based on the clean reactivity observed with  $\text{Ph}_3\text{SiCl}$ , we synthesized a reagent capable of transferring nitrite to **1** by preparing  $\text{Ph}_3\text{Si}(\text{ONO})$  via salt metathesis of  $\text{Ph}_3\text{SiCl}$  and  $\text{AgNO}_2$  in benzene solvent.<sup>17</sup>

The reaction of **1** with  $\text{Ph}_3\text{Si}(\text{ONO})$  occurs immediately in dichloromethane solvent: when  $\text{Ph}_3\text{Si}(\text{ONO})$  is added to a yellow solution of **1**, a rapid color change to green occurs.  $^{19}\text{F}$  NMR spectra of the resulting solution confirm the quantitative formation of  $\text{Ph}_3\text{SiF}$ , indicating metathesis of fluoride. The color change is indicative of oxidation from copper(I) to copper(II), a supposition confirmed by EPR and UV-vis spectra collected of reaction solutions.<sup>18</sup> Solid state IR spectra of the isolated green material from this reaction do not show bands associated with nitrite or a metal–nitrosyl species, however a new ligand  $\text{C}=\text{O}$  stretch at  $1658\text{ cm}^{-1}$  was visualized (consistent with a change in protonation state of the ligand), along with broadened  $-OH$  bands. Based on the above findings, we hypothesized that the terminal copper-containing product in this reaction was a copper(II)–aquo complex ( $\text{Cu}(\text{OH}_2)\text{Hthpa}$ , **2**, Fig. 2).

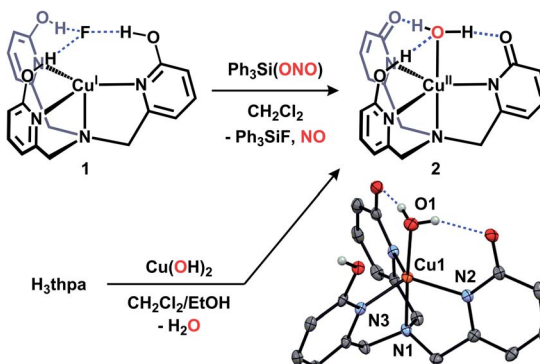


Fig. 2 Syntheses and crystal structure of **2** (thermal ellipsoids shown at 50% probability, H-atoms not involved in H-bonding and solvent omitted for clarity).

We sought an alternative preparation of **2** to confirm its formation during the reaction of **1** with  $\text{Ph}_3\text{Si}(\text{ONO})$ . Authentic samples of complex **2** were prepared by allowing equimolar amounts of the ligand,  $H_3\text{thpa}$ , and  $\text{Cu}(\text{OH})_2$  to react in dichloromethane/ethanol solution. The solution characterization data (UV-vis and EPR) for **2** prepared in this manner were identical to those from the reaction of **1** with  $\text{Ph}_3\text{Si}(\text{ONO})$ .<sup>18</sup> The crystal structure of **2** contains two independent molecules along with an ethanol solvate which is engaged in H-bonding interactions with only one of the molecules. The solid state structure of one of the independent molecules of **2** is presented in Fig. 2 and reveals a trigonal bipyramidal coordination geometry at copper, consistent with the solution state coordination geometry as determined by EPR and UV-vis spectroscopy.<sup>16a,18</sup> The  $\text{Cu}-\text{OH}_2$  is coordinated at a distance of  $1.956(2)$  Å from copper and features H-bonds ( $\text{O}\cdots\text{O}$  separations  $2.567(3)$  and  $2.664(3)$  Å) to the asymmetric Hthpa ligand. The asymmetry of the ligand environment is confirmed by examination of the ligand's C–O bond lengths ( $1.299(3)$  Å and  $1.284(3)$  Å for the deprotonated ‘arms’ and  $1.325(3)$  Å for the protonated ‘arm’) which reflect the anionic nature of the two ligand ‘arms’. The protonated ‘arm’ (N3) is engaged in intermolecular H-bonding interactions with another molecule of **2**, as opposed to the Cu-bound O atom. This network of intermolecular H-bonding, which forms a 1-D chain in the extended structure, is presumably a manifestation of crystal packing and unlikely to persist in solution under dilute conditions.<sup>19</sup>

In addition to the formation of **2** from **1** and  $\text{Ph}_3\text{Si}(\text{ONO})$ , NO was also confirmed as a reaction product by gas-phase IR spectroscopy, as well as by trapping experiments with CoTPP (TPP = tetraphenylporphyrin) and quantification using UV-vis spectroscopy.<sup>20</sup> Headspace analysis of reaction mixtures revealed two broad bands at  $1904$  and  $1844\text{ cm}^{-1}$  in the IR spectrum, consistent with NO, as well as bands associated with dichloromethane solvent vapors (Fig. S12†). To further support the assignment of gaseous NO as a by-product, we prepared the  $^{15}\text{N}$  isotopologue,  $\text{Ph}_3\text{Si}(\text{O}^{15}\text{NO})$ , and allowed it to react with **1**. Headspace analysis of the reaction mixture by IR spectroscopy showed two broad bands at  $1868$  and  $1817\text{ cm}^{-1}$ , consistent with  $^{15}\text{NO}$ , further substantiating NO formation during the



reaction of **1** and  $\text{Ph}_3\text{Si}(\text{ONO})$ . The formation of NO was quantitative, as revealed by CoTPP trapping experiments.

Control reactions confirmed that the quantitative generation of NO was unique to **1**. For instance, to examine whether a direct reaction of the silyl-reagent with a metal fluoride induced NO extrusion, we performed a control experiment where the known copper(i) fluoride  $\text{CuF}(\text{PPh}_3)_3$  (**3**)<sup>21</sup> was allowed to react with  $\text{Ph}_3\text{Si}(\text{ONO})$ .<sup>22</sup> Headspace analysis of this reaction mixture by IR spectroscopy revealed negligible bands associated with NO (Fig. S12†). Trapping experiments with CoTPP did not reveal any significant formation of NO above the background during the reaction of **3** and  $\text{Ph}_3\text{Si}(\text{ONO})$ .

The quantitative yield of NO from complex **1** cannot be attributed solely to a disproportionation reaction of nitrite. Under sufficiently acidic conditions, nitrite disproportionates to form NO, along with other  $\text{NO}_x$  species.<sup>23</sup> To examine a possible acid-promoted nitrite disproportionation pathway that produces NO, we probed the reactivity of  $\text{Ph}_3\text{Si}(\text{ONO})$  with  $\text{CuF}(\text{H}_3\text{thpa})\text{BF}_4$  (**4**).<sup>16b</sup> Complex **4** serves as an ideal platform to test the ability of the ligand framework to deliver  $\text{H}^+$  equivalents to nitrite since (1)  $e^-$  transfer is not possible and (2) the  $-\text{OH}$  groups within the putative  $\text{Cu}(\text{H}_3\text{thpa})^{2+}$  dication are expected to be more acidic than in the analogous  $\text{Cu}(\text{H}_3\text{thpa})^+$  monocation.<sup>24</sup> Although NO was detected by IR spectroscopy in the headspace of reaction samples containing **4** and  $\text{Ph}_3\text{Si}(\text{ONO})$ , quantification using CoTPP revealed formation of NO in only *ca.* 10% yield above the background decomposition.<sup>18</sup> Taken together, these results confirm the necessity of the  $\text{H}_3\text{thpa}$  ligand framework on copper(i) to mediate nitrite reduction in the absence of any exogenous  $\text{H}^+$  source. The quantitative formation of NO from **1** and  $\text{Ph}_3\text{Si}(\text{ONO})$  confirms that **1** serves to deliver  $\text{H}^+$  and  $e^-$ , as opposed to initiating acid-mediated disproportionation.

The generation of a copper(II)– $(\text{OH}_x)$  species from copper(i) and nitrite is reminiscent of a proposed pathway for biological nitrite reduction in CuNiR (Fig. 1B). We sought to investigate key intermediates along the nitrite reduction pathway in our system to provide insight into the reaction sequence that may be applied to CuNiR. However, no intermediates were detected by  $^1\text{H}$  NMR spectroscopy during the reaction of **1** with  $\text{Ph}_3\text{Si}(\text{ONO})$  at or below  $-50^\circ\text{C}$ , which precluded mechanistic analysis in solution.<sup>18</sup> Accordingly, we examined the reaction profile using density functional theory (DFT) calculations.<sup>18</sup> The initial nitrite binding step was first interrogated for a series of possible  $\text{Cu}(\text{H}_3\text{thpa})$ –nitrite adducts. Three nearly isoenergetic ( $<0.5$  kcal mol $^{-1}$  difference) structures were computationally identified that feature an interaction of nitrite with the putative  $\text{Cu}(\text{H}_3\text{thpa})^+$  cation (Fig. S16†).<sup>25</sup> These included an ‘encounter’ complex (**I**, Fig. 3A) where, reminiscent of the  $\text{F}^-$  binding in **1**, nitrite is positioned in the second coordination sphere by H-bonding interactions. Additionally, two other isomers were located containing two nitrite coordination modes; an  $\eta^1\text{-kO}$  isomer (**I'**) and an  $\eta^1\text{-kN}$  isomer (**I''**, Fig. S16†).

The nitrite reduction sequence subsequent to the initial binding event was evaluated. In analogy to Fig. 1A, nitrite reduction *via* water elimination from the  $\eta^1\text{-kN}$  isomer (**I''**) to provide a copper-nitrosyl (**III**, Scheme S2†) was found to be an

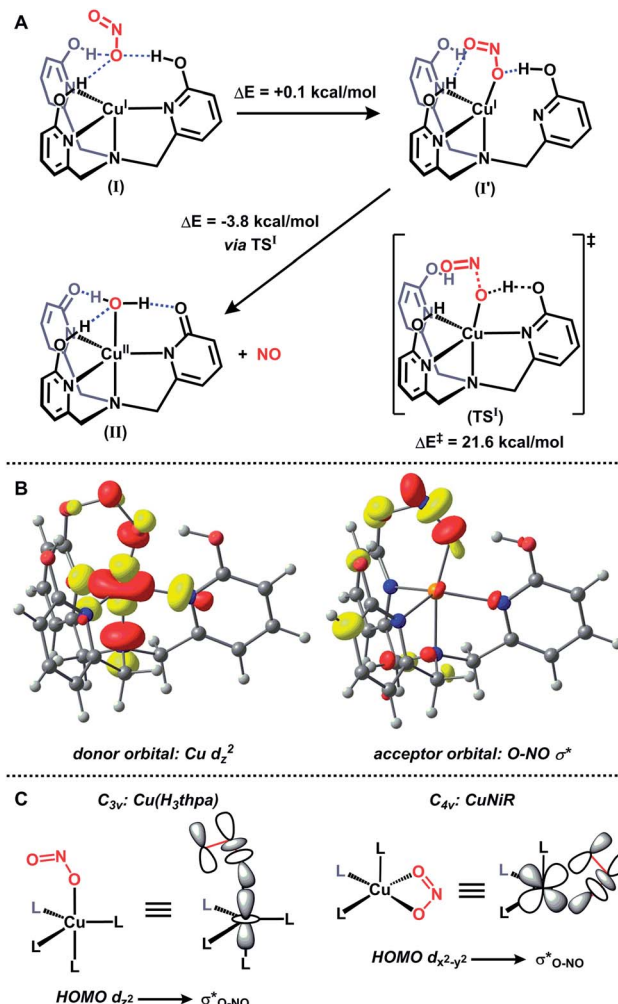


Fig. 3 DFT-calculated pathway for nitrite reduction (a), donor and acceptor molecular orbitals along the N–O bond cleavage reaction coordinate (b, isovalue = 0.05) and comparison of nitrite binding mode and donor/acceptor orbitals for  $\text{Cu}(\text{H}_3\text{thpa})^+$  (c, left) and CuNiR (c, right).

endothermic process by 17.9 kcal mol $^{-1}$ , presumably due to the formation of a high energy copper(II)–nitrosyl (Fig. S17†). In contrast, and in analogy to Fig. 1B, reduction *via* NO elimination from the  $\eta^1\text{-kO}$  isomer (**I'**) was found to be an exothermic process by 3.8 kcal mol $^{-1}$  to generate the experimentally observed copper(II)–aquo (**II**) species (Fig. 3A).

The transition state for the critical N–O bond breaking step (**TS<sup>I</sup>**) was located computationally and is 21.6 kcal mol $^{-1}$  above the starting ‘encounter’ complex **I**. In the calculated transition state **TS<sup>I</sup>**,  $\text{H}^+$  transfer from the  $\text{H}_3\text{thpa}$  scaffold to the coordinated nitrite is accompanied by elongation of the O–NO bond. There is substantial Mulliken spin density on the Cu–O fragment (0.565) in the transition state. This value is intermediate between the Mulliken spin density of the starting species **I** (0.0) and the Mulliken spin density on the Cu–O fragment in the product **II** (0.929). The spin density on the Cu–O fragment in the transition state (along with spin density of the opposite sign on NO, Fig. S19†) indicates charge transfer from copper to nitrite concomitant with  $\text{H}^+$  transfer from  $\text{H}_3\text{thpa}$  to nitrite. This  $\text{H}^+/\text{e}^-$



transfer, accompanied by NO ejection, is followed by an additional  $\text{H}^+$  transfer from the  $\text{H}_3\text{thpa}$  ligand to copper-bound hydroxide to form the final copper(II)-aquo product **II**.

To understand the impact of the binding mode of nitrite in our system as compared to CuNiR we analyzed the frontier molecular orbitals of structures along the O-NO bond cleavage reaction coordinate. The empty  $\sigma_{\text{O-NO}}^*$  orbital overlaps with the filled Cu  $d_{z^2}$  orbital (Fig. 3B). This is in contrast to CuNiR, where the highest occupied molecular orbital (HOMO) is primarily  $d_{x^2-y^2}$  character and subsequently nitrite coordinates in a bidentate manner to maximize orbital overlap between  $d_{x^2-y^2}$  and  $\sigma_{\text{O-NO}}^*$  for electron transfer.<sup>10</sup> For  $\text{Cu}(\text{H}_3\text{thpa})^+$ , the HOMO is  $d_{z^2}$  and favors an alternative mode of nitrite binding. The binding of nitrite as a monodentate ligand  $\kappa\text{O}$  maximizes overlap between  $d_{z^2}$  and  $\sigma_{\text{O-NO}}^*$  for electron transfer (Fig. 3C). The  $d_{z^2}$  ground state predicted for **II**, subsequent to electron transfer and NO release, is in agreement with the experimental EPR data for **2**.<sup>16a,b,18</sup>

The difference in mode of nitrite binding between our synthetic system and CuNiR has ramifications on the calculated barrier height for O-NO bond cleavage. In CuNiR, bidentate coordination of nitrite to copper maximizes back-bonding interactions and significantly lowers the calculated barrier to O-NO bond cleavage (16 kcal mol<sup>-1</sup>).<sup>10</sup> When a monodentate coordination was examined *in silico*, the extent of back-bonding between copper and nitrite was significantly lower and consequently, a higher barrier to O-NO bond cleavage was observed (26 kcal mol<sup>-1</sup>).<sup>10</sup> The barrier in the present system (21 kcal mol<sup>-1</sup>) is intermediate of these regimes in CuNiR. The H-bonding interactions in **TS<sup>I</sup>** between the distal oxygen of the nitrite anion and the  $-OH$  groups of the  $\text{H}_3\text{thpa}$  ligand serves to lower the  $\sigma_{\text{O-NO}}^*$  orbital energy, similar in fashion to bidentate coordination to copper. In contrast to energetic consequences on orbital energies imposed by geometric constraints, the hydrogen bonding interactions in  $\text{H}_3\text{thpa}$  provide an alternative means by which to lower the  $\sigma_{\text{O-NO}}^*$  orbital energy, and this approach may well be exploited as a general strategy to minimize energetic costs associated with substrate reduction. Such strategies have been thoroughly described for biological systems.<sup>26</sup>

## Conclusions

In conclusion, we have demonstrated nitrite reduction by a copper complex featuring a proton-responsive tripodal ligand. The formation of NO was confirmed by gas-phase IR spectroscopy, isotope labelling, and trapping experiments. DFT calculations predict that nitrite binds in an  $\eta^1\kappa\text{O}$  fashion to the copper center prior to reduction *via* a  $\text{H}^+/\text{e}^-$  transfer. This reaction, facilitated by the secondary sphere environment, parallels the crucial role of H-bonding residues near the active site of CuNiR, which serve to position nitrite and facilitate electron transfer. This is, to our knowledge, the first synthetic copper system to reduce nitrite in such a fashion.<sup>27</sup> Ongoing efforts on this system are focused at utilizing the  $\text{H}_3\text{thpa}$  scaffold to facilitate multiple  $\text{H}^+/\text{e}^-$  transfer events to coordinated substrates.

## Acknowledgements

This work was supported by the University of Michigan Department of Chemistry, NSF-GRFP (CMM), UM Rackham Graduate School (CMM), NSF grant CHE-0840456 for X-ray instrumentation and through computational resources and services provided by Advanced Research Computing at UM. NKS is a Dow Corning Assistant Professor and Alfred P. Sloan Research Fellow. We thank Dr Jeff W. Kampf for X-ray assistance and Prof. Nicolai Lehnert and Prof. Abhishek Dey for helpful discussions.

## Notes and references

- (a) B. A. Averill, *Chem. Rev.*, 1996, **96**, 2951; (b) W. G. Zumft, *Microbiol. Mol. Biol. Rev.*, 1997, **61**, 533; (c) A. C. Merkle and N. Lehnert, *Dalton Trans.*, 2012, 3355 and references therein.
- S. Suzuki, K. Kataoka, K. Yamaguchi, T. Inoue and Y. Kai, *Coord. Chem. Rev.*, 1999, **190-192**, 245.
- (a) M. E. P. Murphy, S. Turley and E. T. Adman, *J. Biol. Chem.*, 1997, **272**, 28455; (b) M. J. Ellis, M. Prudencio, F. E. Dodd, R. W. Strange, G. Sawers, R. R. Eady and S. S. Hasnain, *J. Mol. Biol.*, 2002, **316**, 51; (c) S. V. Antonyuk, R. W. Strange, G. Sawers, R. R. Eady and S. S. Hasnain, *Proc. Natl. Acad. Sci. U. S. A.*, 2005, **102**, 12041.
- B. A. Averill, *Angew. Chem., Int. Ed.*, 1994, **33**, 2057.
- E. I. Tocheva, F. I. Rosell, A. G. Mauk and M. E. P. Murphy, *Science*, 2004, **304**, 867.
- Note that the NO adduct of reduced CuNiR can also be generated in solution, see: O. M. Usov, Y. Sun, V. M. Grigoryants, J. P. Shapleigh and C. P. Scholes, *J. Am. Chem. Soc.*, 2006, **128**, 13102.
- (a) C. L. Hulse, J. M. Tiedje and B. A. Averill, *J. Am. Chem. Soc.*, 1989, **111**, 2322; (b) M. Sarma and B. Mondal, *Inorg. Chem.*, 2011, **50**, 3206.
- K. Kataoka, H. Furusawa, K. Takagi, K. Yamaguchi and S. Suzuki, *J. Biochem.*, 2000, **127**, 345.
- (a) Y. Zhao, D. A. Lukyanov, Y. V. Toropov, K. Wu, J. P. Shapleigh and C. P. Scholes, *Biochemistry*, 2002, **41**, 7464; (b) S. Suzuki, K. Kataoka and K. Yamaguchi, *Acc. Chem. Res.*, 2000, **33**, 728; (c) K. Kobayashi, S. Tagawa, Deligeer and S. Suzuki, *J. Biochem.*, 1999, **126**, 408.
- S. Ghosh, A. Dey, Y. Sun, C. P. Scholes and E. I. Solomon, *J. Am. Chem. Soc.*, 2009, **131**, 277.
- For select Cu(II) examples, see: (a) F. Hueso-Ureña, A. L. Peñas-Chamorro, M. N. Moreno-Carretero, M. Quirós-Olozabal and J. M. Salas-Peregrín, *Polyhedron*, 1999, **18**, 351; (b) M. Harata, K. Jitsukawa, H. Masuda and H. Einaga, *Bull. Chem. Soc. Jpn.*, 1998, **71**, 637.
- Note that copper(I)-nitrite adducts featuring  $\kappa\text{O}$ -coordination have been observed using phosphine ligands, see: J. A. Halfen and W. B. Tolman, *Acta Crystallogr., Sect. C: Cryst. Struct. Commun.*, 1995, **51**, 215, along with ref. 13d and 13e.
- For selected examples, see: (a) J. A. Halfen, S. Mahapatra, M. M. Olmstead and W. B. Tolman, *J. Am. Chem. Soc.*, 1994, **116**, 2173; (b) J. A. Halfen, S. Mahapatra,



E. C. Wilkinson, A. Gengenbach, V. G. Young Jr, L. Que and W. B. Tolman, *J. Am. Chem. Soc.*, 1996, **118**, 763; (c) J. A. Halfen and W. B. Tolman, *J. Am. Chem. Soc.*, 1994, **116**, 5475; (d) W.-J. Chuang, I. J. Lin, H.-Y. Chen, Y.-L. Chang and S. C. N. Hsu, *Inorg. Chem.*, 2010, **49**, 5377; (e) S. C. N. Hsu, Y.-L. Chang, W.-J. Chuang, H.-Y. Chen, I. J. Lin, M. Y. Chiang, C.-L. Kao and H.-Y. Chen, *Inorg. Chem.*, 2012, **51**, 9297; (f) M. Kujime and H. Fujii, *Angew. Chem., Int. Ed.*, 2006, **45**, 1089; (g) P. P. Paul and K. D. Karlin, *J. Am. Chem. Soc.*, 1991, **113**, 6331.

14 (a) M. Sarma, A. Kalita, P. Kumar, A. Singh and B. Mondal, *J. Am. Chem. Soc.*, 2010, **132**, 7846; (b) M. Sarma, A. Singh, G. S. Gupta, G. Das and B. Mondal, *Inorg. Chim. Acta*, 2009, **363**, 63.

15 A. M. Wright, G. Wu and T. W. Hayton, *J. Am. Chem. Soc.*, 2010, **132**, 14336.

16 (a) C. M. Moore, D. A. Quist, J. W. Kampf and N. K. Szymczak, *Inorg. Chem.*, 2014, **53**, 3278; (b) C. M. Moore and N. K. Szymczak, *Chem. Commun.*, 2015, **51**, 5490.

17 For a similar synthesis to generate  $\text{Si}^i\text{Pr}_3(\text{ONO})$ , see: M. Weidenbruch and F. Sabeti, *Z. Naturforsch., B: Anorg. Chem., Org. Chem.*, 1976, **31**, 1212.

18 See the Electronic ESI† for more details.

19 DFT optimizations of **2** using a  $\text{CH}_2\text{Cl}_2$  dielectric predict that all OH groups engage in intramolecular H-bonding interactions. Under dilute conditions where intermolecular interactions are less favored, we presume this is an accurate depiction of the solution structure and have therefore represented **2** in accordance with the computational results.

20 M. Kumar, N. A. Dixon, A. C. Merkle, M. Zeller, N. Lehnert and E. T. Papish, *Inorg. Chem.*, 2012, **51**, 7004.

21 F. H. Jardine, L. Rule and A. G. Vohra, *J. Chem. Soc. A*, 1970, 238.

22  $\text{CuF}(\text{PPh}_3)_3$  was selected as a viable copper(i) fluoride given its reported synthesis and characterization, in contrast to  $\text{CuF}(\text{tpa})$ , which is not known. See ref. 16b.

23 M. S. Rayson, J. C. Mackie, E. M. Kennedy and B. Z. Dlugogorski, *Inorg. Chem.*, 2012, **51**, 2178.

24 Note that  $\text{CuCl}(\text{H}_3\text{thpa})$  (see ref. 16a) can be deprotonated with weak bases such as sodium acetate, suggesting an upper limit for the first  $\text{p}K_a$  of  $\text{CuX}(\text{H}_3\text{thpa})$  complexes is ~4. Please see the ESI† for more details.

25 Note that the presence of nearly isoenergetic coordination isomers is in accordance with previous studies on copper-nitrite adducts, see: N. Lehnert, U. Cornelissen, F. Neese, T. Ono, Y. Noguchi, K. Okamoto and K. Fujisawa, *Inorg. Chem.*, 2007, **46**, 3916.

26 (a) G. A. Jeffery and W. Saenger, *Hydrogen Bonding in Biological Structures*, Springer-Verlag, Berlin, 1991; (b) K. M. Lancaster, *Struct. Bonding*, 2012, **142**, 119.

27 Note that a similar mechanism for iron-mediated nitrite reduction was recently reported, see: E. M. Matson, Y. J. Park and A. R. Fout, *J. Am. Chem. Soc.*, 2014, **136**, 17398.

